FOSTER, S., MUHAMMAD-SUKKI, F., RAMIREZ-INIGUEZ, R., RAINE, D.F., DECIGA-GUSI, J., ABU-BAKAR, S.H., BANI, N.A., MUNIR, A.B., MAS'UD, A.A. and ARDILA-REY, J.A. 2020. Assessment of the RACPC performance under diffuse radiation for use in BIPV system. *Applied sciences* [online], 10(10), article ID 3552. Available from: https://doi.org/10.3390/app10103552

Assessment of the RACPC performance under diffuse radiation for use in BIPV system.

FOSTER, S., MUHAMMAD-SUKKI, F., RAMIREZ-INIGUEZ, R., RAINE, D.F., DECIGA-GUSI, J., ABU-BAKAR, S.H., BANI, N.A., MUNIR, A.B., MAS'UD, A.A. and ARDILA-REY, J.A.

2020

applied sciences

MDPI

Communication

Assessment of the RACPC Performance under Diffuse Radiation for Use in BIPV System

Stephania Foster [1], Firdaus Muhammad-Sukki [2,*], Roberto Ramirez-Iniguez [1,*], Daria Freier Raine [1], Jose Deciga-Gusi [1], Siti Hawa Abu-Bakar [3], Nurul Aini Bani [4], Abu Bakar Munir [5], Abdullahi Abubakar Mas'ud [6] and Jorge Alfredo Ardila-Rey [7]

1 School of Computing, Engineering and Built Environment, Glasgow Caledonian University, Cowcaddens Road, Glasgow, Scotland G4 0BA, UK; stephania.foster@outlook.com (S.F.); daria_freier@outlook.de (D.F.R.); jdecig200@caledonian.ac.uk (J.D.-G.)
2 School of Engineering, Robert Gordon University, Garthdee Road, Aberdeen, Scotland AB10 7GJ, UK
3 Renewable Energy Research Laboratory, Electrical Engineering Section, British Malaysian Institute, Universiti Kuala Lumpur, Jalan Sungai Pusu, Selangor 53100, Malaysia; hawa012@gmail.com
4 UTM Razak Faculty of Technology and Informatics, Universiti Teknologi Malaysia, Jalan Sultan Yahya Petra, Kuala Lumpur 54100, Malaysia; nurulaini.kl@utm.my
5 Eversheds Harry Elias, SGX Centre 2, #17-01, 4 Shenton Way, Singapore 068807, Singapore; munirapac@eversheds-harryelias.com
6 Department of Electrical and Electronics Engineering, Jubail Industrial College, P O Box 10099, Jubail 31961, Saudi Arabia; masud_a@jic.edu.sa
7 Department of Electrical Engineering, Universidad Técnica Federico Santa María, Santiago de Chile 8940000, Chile; jorge.ardila@usm.cl
* Correspondence: f.b.muhammad-sukki@rgu.ac.uk (F.M.-S.); rra4@gcu.ac.uk (R.R.-I.)

Received: 29 April 2020; Accepted: 19 May 2020; Published: 21 May 2020

Featured Application: Alternative Solar Photovoltaic; Building Integrated Photovoltaic.

Abstract: In the last four decades there has been a significant increase in solar photovoltaic (PV) capacity, which makes solar one of the most promising renewable energy sources. Following this trend, solar power would become the world's largest source of electricity by 2050. Building Integrated Photovoltaic (BIPV) systems, in which conventional materials can be replaced with PV panels that become an integral part of the building, can be enhanced with concentrating photovoltaic (CPV) systems. In order to increase the cost efficiency of a BIPV system, an optical concentrator can be used to replace expensive PV material with a lower cost option, whilst increasing the electrical output through the concentration of solar power. A concentrator called rotationally asymmetrical compound parabolic concentrator (RACPC) was analysed in this work under diffuse light conditions. Software simulations and experimental work were carried out to determine the optical concentration gain of the concentrator. Results from this work show that, under diffuse light, the RACPC has an optical concentration gain of 2.12. The experimental work showed a value of 2.20, which confirms the results with only a 3.8% difference.

Keywords: solar photovoltaic; building integrated photovoltaic systems; rotationally asymmetrical compound parabolic concentrator; diffuse radiation

1. Introduction

A significant amount (around 40%) of the energy usage worldwide is consumed by buildings. The necessity of transforming buildings from energy users to energy producers has motivated an increase in renewable energy's share of global energy consumption [1–6]. Building integrated photovoltaic

(BIPV) systems integrate photovoltaic panels into buildings as windows, façades or roofs by replacing conventional materials and producing renewable electricity onsite. The cost-effectiveness of the system comes from the considerable savings in terms of material costs, electricity, and improvements to the buildings' energy performance [7–9]. Figure 1 shows some of the BIPV implementations.

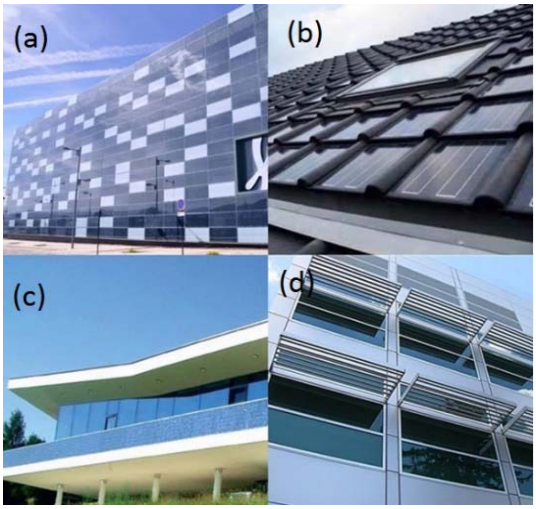

Figure 1. Building integrated photovoltaic (BIPV) integration in (**a**) facade; (**b**) rooftop; (**c**) spandrels and parapets; (**d**) sun shading. Reproduced from [8,10,11].

BIPV systems have been implemented in different places around the world proving their benefits. This has motivated projects developers, investors and architects to include this type of system in their building planning. In Mexico City a BIPV system was implemented with a photovoltaic (PV) skylight in a shopping centre, which prevented the release of 233 tons of CO_2 into the atmosphere and with a payback of less than a year. In Honolulu there is another example where a photovoltaic canopy was implemented into a building generating 58,000 kWh per year, this being enough power to feed 3300 lights in the building and prevent the release of 38 tons of CO_2 into the atmosphere [12]. Therefore, different targets regarding building energy efficiency have been created. In the United Kingdom, the "Nearly Zero-Energy Buildings" of the Energy Performance of Building Directive (EPBD) [13] seeks to achieve that all new domestic buildings meet a Zero Carbon Standard. In the USA the "Net Zero Energy Building" introduces the BIPV as an ambitious system which needs to be implemented in all new buildings with the aim of fulfilling the set standards for every building of energy neutrality [4]. A Nearly (or Net) Zero Energy Building is a building with a high energy performance. It can generate its own energy on-site or nearby—typically via renewable sources—to meet all its annual energy requirements.

A major issue for the PV industry and hence to the BIPV sector, is to offer customised products at a competitive price. Certainly, the most expensive part of a solar PV system is the PV cells, which represent between 40% and 50% of the total cost [14]. Therefore, the PV and BIPV industries seek to achieve an increase in the efficiency of the system at an affordable price. They seek to improve existing technologies and bring the development of new technologies together with conventional building materials to serve as an intelligent, multifunctional compound [4]. The concentrating photovoltaic (CPV) system is one of the most recent technological advances proposed to achieve this goal, since it replaces the solar cell material with a cheaper material of which the optical concentrator is made. To date, several types of CPV systems have been investigated incorporating many concentrator designs such as variations of compound parabolic concentrators (CPCs) [15–19], variations of dielectric totally internally reflecting concentrators (DTIRCs) [20,21], luminescent solar concentrators (LSCs) [22,23], etc.

Sarmah et al. [24] studied the performance of an asymmetric CPC-PV and tested it indoor. He found that his concentrating module could achieve a maximum electrical conversion efficiency

of 12.1%. In terms of cost per unit power output, the CPV module could achieve a 20% reduction when compared with a non-concentrating counterpart. Mallick and Eames [25] tested the prototype of a solar concentrator module consisting of a different asymmetric CPC design for building façade integration. The CPV module achieved an electrical conversion efficiency of 10.2% when tested indoor and could achieve a potential cost reduction of 40% per m^2 under mass production when compared with a standard PV panel. Dayanand et al. [26] evaluated the performance on the absorptive/reflective CCPC (AR-CCPC) module mounted on the roof top of the Heriot-Watt University building in Dubai, and found that such system is capable of achieving an overall electrical conversion efficiency of 15%.

Abu-Bakar et al. [27] developed a CPV window incorporating rotationally asymmetrical dielectric totally internally reflecting concentrators. The CPV window was tested indoor and generated a maximum power of 0.749 W at normal incidence, 4.8 × higher than the non- concentrating PV window. Marín-Sáez et al. [28] simulated the energy generated from a holographic concentrating PV-thermal (PVT) system integrated in a building in Avignon, France. The simulations indicated that such system is capable of achieving an optical efficiency of 43% and can provide 9.1% of the electricity demand of the building. Timmermans et al. [29] studied the performance of the smart window created from the LSC using two types of dye tested at different temperatures. At 25 °C, the LSC obtained a maximum electrical efficiency of 3%. Aghaei et al. [30] on the other hand, simulated the performance of an LSC coupled with bifacial PV solar cells made of mono-crystalline silicon. Their simulation achieved an electrical conversion efficiency of 16.9% under standard test conditions (STC). Table 1 summarises all the CPV work discussed previously.

Table 1. Summary of concentrating photovoltaic (CPV) research.

Authors	Type of Concentrator	Configuration	Findings
Sarmah et al. [24]	Asymmetric compound parabolic concentrator	Building façade	Achieved an electrical conversion efficiency of 12.1%. In terms of cost per unit power output, the CPV module could achieve a 20% reduction when compared with a non-concentrating counterpart.
Mallick and Eames [25]	Asymmetric compound parabolic concentrator	Building façade	Achieved an electrical conversion efficiency of 10.2% when characterised outdoors. Potential cost reduction of 40% per m^2 under mass production when compared to similar PV module.
Dayanand et al. [26]	Cross-compound parabolic concentrator	Roof mounted	Achieved an overall electrical conversion efficiency of 15%.
Abu-Bakar et al. [27]	Rotationally asymmetrical dielectric totally internally reflecting concentrators	Window	Generated 0.749 W at normal incidence, 4.8 × higher than the non- concentrating PV.
Marín-Sáez et al. [28]	Holographic	Integrated as building blinds	Achieved optical efficiency of 43%. Generate 9.1% of electricity requirement of the building.
Timmermans et al. [29]	Luminescent solar concentrator	Window	Achieved an overall electrical conversion efficiency of 3%.
Aghaei et al. [30]	Luminescent solar concentrator	n/a	Obtained an electrical conversion efficiency of 16.9% under standard test conditions (STC).

However, in order to maximise the electricity generation, a single or double-axis sun-tracking system is normally required on a CPV module; in addition, depending on the design, a cooling system might be required. This increases the prices when compared with a conventional PV system; although the higher efficiency and the savings on PV material may eventually compensate the costs [31]. Due to the fact that the majority of the optical concentrators are designed to work under direct solar irradiation, it has been believed that the CPV systems need to be used in locations with high direct solar irradiation for a good performance [31]. However, diffuse solar irradiation also has an impact on the performance of the concentrator; and this needs to be evaluated.

The main objective of this paper is to analyse and determine the concentrator's behavior under overcast daytime conditions, which has never been explored before. An optical analysis software is used to determine the output of the system under diffuse light radiation and the results are compared to the output obtained from the fabricated sample tested through an outdoor experiment. This paper is structured as follows: Section 1 is the introduction, Section 2 defines the concentrator used in this work—the rotationally asymmetrical compound parabolic concentrator, Section 3 describes the simulation work while Section 4 explains the fabrication, the experimental setup and the results, and finally Section 5 concludes the paper.

2. Novel Rotationally Asymmetrical Compound Parabolic Concentrator (RACPC)

A concentrator called rotationally asymmetrical compound parabolic concentrator (RACPC) was developed by Abu-Bakar et al. [32]. The design algorithm was implemented in software by using MATLAB®. The design software requires the following input parameters: the index of refraction of the concentrator's material (n), the total height of the concentrator (H_{tot}), the length of the PV cell (L_{PV}), the half- acceptance angle (θ_a), the width of the PV cell (W_{PV}), the number of extreme rays (N); and the trial width of the entrance aperture (d_1) [32].

A 2D symmetrical design is first produced using the input parameters as is shown in Figure 2. The first 2D symmetrical design is created at position "1" by defining the coordinates of the side wall of the parabola and calculating the trial height taking into account that a number of extreme rays enter the concentrator at the critical angle. Second, the software compares the calculated entrance aperture with the trial entrance aperture; and using the different between the two apertures it adjusts the trial entrance aperture until after several iterations an acceptable error value is achieved [32]. Then, for the total height of the concentrator a similar process takes place, the difference between the calculated total height is compared with the desired total height and adjusted by varying the "trial" half-acceptance angle until an acceptable error value is reached. For the position "2" (Figure 2) the process is repeated [32].

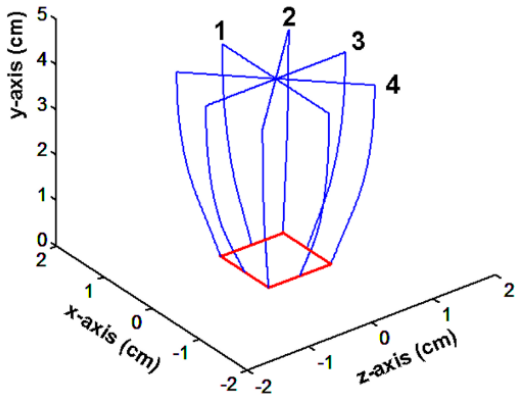

Figure 2. Demonstration of the angular rotation of the 2-D cross-sections to produce the rotationally asymmetrical compound parabolic concentrator (RACPC) [33].

The new design is computed by incrementing the angle of rotation of the cross section by 1°; and when an 180° rotation around the y-axis is completed, the process stops. Thus, the following three output parameters are obtained: the final width of the entrance, the final half-acceptance angle and the geometrical concentration gain of the concentrator [32].

The advantages of the RACPC in comparison with a conventional CPC designs include [32]: (i) the flat entrance aperture of the RACPC helps to mould arrays of these concentrators, with a thin layer of the same material joining them together thus reducing the assembly cost of the system; (ii) the square exit aperture allows for the solar cell to be easily attached, and (iii) due to the concentration

provided on both planes perpendicular to the propagation of light along the concentrator axis and a higher geometrical concentration gain, it can be considered as a 3D design.

The detail design process, variation of RACPC designs, and extensive simulations to determine the optical concentration gain of each RACPC designs under direct irradiance has been explored in detail by Abu-Bakar et al. in [32]. They found that the RACPC can achieve the maximum optical concentration gain value of 6.2 for a 5 cm tall RACPC design. One specific design of RACPC-PV that has a total height of 3 cm was fabricated and tested indoor to verify its performance under direct irradiance [18]. A square PV cell of 1 cm sides was attached to the RACPC. The test which was carried out under standard test conditions (Irradiance of 1000 W/m^2, temperature of 25 °C and A.M. 1.5 G) demonstrated a greater maximum power output when compared with a similar size non-concentrating PV cell; achieving a gain of 3.33.

However, diffuse solar irradiation also has an impact on the performance of the concentrator; particularly in countries at a higher latitude. So far, the performance of RACPC under diffuse radiation has never been investigated. The aim of this paper is to analyse and determine the concentrator's behavior under overcast day conditions. This will improve the overall understanding of overall the performance of this concentrator under direct and diffuse irradiance.

3. Simulation Performance Analysis

Prior to carrying out the performance evaluation through an outdoor experiment, the electrical output generated from the RACPC prototype under diffuse conditions was predicted through an optical concentration analysis. According to the optical concentration gain definition, the optical gain can be expressed in the same way as the opto-electronic gain using the total power at the detector with and without an optical concentrator.

$$C_{op-elct} = \frac{P_{\,with\ OC}}{P_{\,without\ OC}} \tag{1}$$

However, the optical losses are included due to the definition of the optical concentration gain. The analysis evaluates the gain performance of the RACPC when it is exposed to rays coming from all directions by a light source, in this case, a dome with a thickness of 1 mm and a 380 mm radius. The dome was created by Freier [34] using AutoCAD and then it was imported into an optical analysis software called ZEMAX®. Figure 3 shows the created ray source.

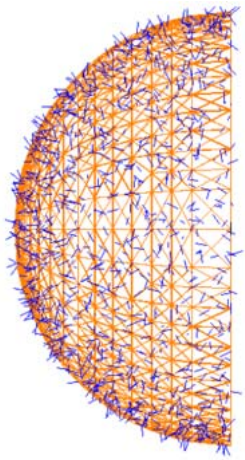

Figure 3. Light source for diffuse light analysis.

The dome shape was implemented with the aim of simulating diffuse light conditions. For this purpose, 1 million rays were emitted by the source at a power of 1000 W. The detector size was 100 mm^2. A layer of index matching gel and the concentrator are positioned inside the dome with a distance

between the dome and the concentrator of 350 mm as illustrated in Figure 4 where the concentrator is displayed in black and orange respectively.

Diffuse light is characterised by rays coming also from the side profile of the concentrator, however, even with the additional rays, the optical concentration gain is lower than that of the direct light simulation performed by Abu-Bakar et al. [32] who achieved an optical concentration gain of 3.34 while the optical gain for diffuse light is 2.12.

The optical efficiency for diffuse light of 58% was calculated using the optical concentration gain definition (Equation (1)). However, for an optical efficiency value, the rays must come only through the entrance aperture not from the sides as it was calculated.

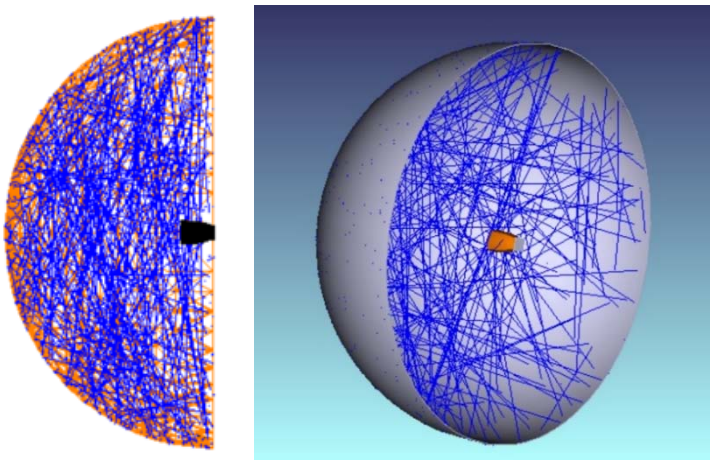

Figure 4. Simulation setup for diffuse analysis; side view (**left**), and isometric view (**right**).

4. Experimental Performance Analysis

In order to know the performance of the concentrator under real diffuse light the next step of the analysis must be performed in an open environment.

4.1. Fabrication of the RACPC-PV Cell

A flat lead wire of 1 mm width and 0.1 mm thickness was used to tab the solar cell on the edge to maximise the active area; the soldering iron rod with a power of 81 W is heated to 350 °C and must be controlled since the high temperature can damage the solar cell. However, before the soldering process, the components should be clean and free from grease. Once they have been cleaned a liquid flux is applied to both ends of the connector to remove oxidation that prevents solder from bonding to metals and thus, having more effective use of the soldering material. Then, one of the ends of the connector piece is connected to the back of the solar cell (positive side) and soldered. It is important to clarify that the amount of soldering material used can increase the resistance of the circuit thus affecting the efficiency.

A standard superglue was used to glue the PV circuit on a glass plate of 70 mm × 70 mm × 40 mm used in controlled amounts in order to avoid flood or overflowing the solar cell and thus generating damage on it. Then, the RACPC can be attached to the PV cell using an encapsulation material which functions simultaneously as an adhesive and as an index matching gel [34]. It is important to mention that the selection of the encapsulation material is a main factor in order to ensure the correct operation of the optical concentrator, as the refraction may be affected by the obstruction of the sunlight flow from the optical concentrator to the solar cell. Sylgard® 184 Silicone Elastomer (Dow Chemical Company Ltd., Dewsbury, UK) provides a good transmission and has an index of refraction of 1.4225. Knowing that the refraction index of the silicon is 3.8821 and for the concentrator it is 1.49, the refractive index of the encapsulation material is not ideal because the value is not the same or close to one of the components of the system, hence, optical losses are expected due to reflection at the borders [34].

One of the important steps of mounting the RACPC on the solar cell is the preparation of the index matching gel as it may affect the performance of the system. However, with the aim of ensuring a better adhesion between the silicon and the cell, Dow Corning Primer 92-023 (Dow Chemical Company Ltd., Dewsbury, UK) was applied to the solar cell leaving it to dry for 10 min. Once the cleaning was completed, a small beaker was used to prepare the Sylgard-184® by mixing in a 10:1 weight ratio and stirred for 10 min. The bubbles in the solution can generate dispersion inside the RACPC reducing the number of photons traveling through the PV material. Therefore, in order to reduce losses, a Heraeus Vacutherm™ vacuum chamber (Heraeus Holding GmbH, Hanau, Germany) was used to eliminate any air bubbles present in the solution working with a pressure of 400 bars at 23.9 °C (as shown in Figure 5) for 15 min. Then, using a painting brush, the index matching gel was spread over the surface and the RACPC was finally placed on the PV cell with precaution. It is important to be precise in order to prevent misalignment between the solar cell and the RACPC leading to significant optical losses. The sample was cured for 48 h at room temperature.

Figure 5. The RACPC-photovoltaic (PV) cell on the glass substrate and the Sylgard-184® solution in a beaker (left), and the Heraeus Vacutherm™ vacuum chamber to eliminate the air bubble (right).

4.2. Experimental Setup and Results

The following equipment was used: (1) an RACPC-PV device and a single PV cell device, where each device uses a 1 cm by 1 cm PV cell; (2) inclinometer; (3) two multimeters, and (4) a digital slope meter. The single cell and the concentrator were connected to different multimeters to get simultaneous readings. The temperature depends on the day on which the experiment was carried out. The sun angle was obtained from www.suncalc.org; and with a digital slope meter the ideal inclination towards the south was setup each day in order to maximise the electrical output.

The outdoor experiment was carried out on the roof of the EA building of Glasgow Caledonian University (GCU) (N 55°51′57.71″, W 4°15′00.49″). This location was selected for two reasons: the first one has to do with the Sky View Factor (SVF), which is a dimensionless parameter and represents the fraction of the visible sky on a hemisphere that lay centred over the selected location. The SVF has values between zero and one; thus, an SVF of one means the complete sky is visible and neither reflected short-wave radiation or additional long-wave radiation is received [35]. The SVF value for the selected site is 0.774 and is shown in Figure 6.

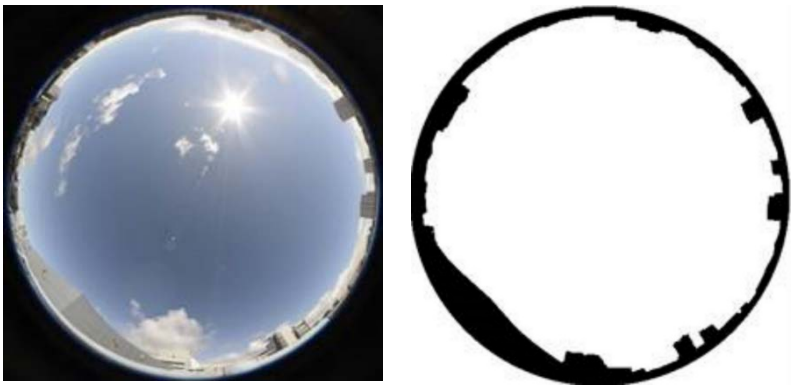

(**a**) (**b**)

Figure 6. (**a**) EA building of Glasgow Caledonian University (GCU) (N 55°51′57.71″, W 4°15′00.49″) and (**b**) SVF = 0.774.

The second reason is that the wireless weather station of the GCU is located in the same place. The Integrated Sensor Suite (ISS) and the Vantage Pro2 console are the two components of the weather station. The first one manages the external sensor array and the second one provides the user interface, data display, and calculation [36]. The weather station also includes the solar radiation sensor and the UV sensor, thus providing relevant information such as temperature, wind speed, and the global irradiance every 15 min, which are required in order to calculate the exact amount of diffuse and direct light when the sun angle is known. Therefore, the calculation of reflected irradiation will not take place as it was not considered necessary.

The experiment was performed on the 15th of March 2017 from 9:00 a.m. to 15:30 p.m. with a temperature of 11.9 °C; and an inclination of 31.96° facing south. The short circuit currents from the RACPC-PV device and the bare PV cell were measured every 15 min, and using the empirical functions shown below, the global irradiation was separated into direct and diffuse irradiation through the k_T factor. This takes into account the global irradiance $E_{G,hor}$, the extra-terrestrial irradiance E_0 that depends on the distance between the sun and the earth and is the irradiance before reaching the atmosphere (the average value is 1361 W/m^2) and the sun height γ_s [37] for each specific time.

$$k_T = \frac{E_{G,hor}}{E_0 \times \sin \gamma_S} \tag{2}$$

where $k_T \rightarrow 0$ means overcast and $k_T \rightarrow 1$ means clear days. The k_T value of the experiment was between 0.14 and 0.44 confirming that the diffuse light was high during the period of the experiment. The diffuse irradiance at the horizontal plane is calculated depending of the value obtained previously due to the fact that the equation varies according to it [37]. Both the k_T and the diffuse irradiance at the horizontal plane values during the experiment are presented in Figure 7.

$$E_{diff,\,hor} = E_{G,hor} \times (1.020 - 0.254 \times k_T + 0.0123 \times \sin \gamma_S) \quad \text{for } k_T \leq 0.3 \tag{3}$$

$$E_{diff,hor} = E_{G,hor} \times (1400 - 1749 \times k_T + 0.177 \times \sin \gamma_S) \quad \text{for } 0.3 < k_T < 0.78 \tag{4}$$

For a measured global irradiance of 1106 Wh/m^2 between 9:00 a.m. and 15:30 p.m., a diffuse irradiance of 1010 Wh/m^2 was calculated for the first experiment, i.e., this means 8.7% of direct irradiance for that period of time of the experiment.

The opto-electronic gain obtained from the outdoor experiment is 2.20 (Figure 8). Note that between 13:00 p.m. and 14:00 p.m., there was a fluctuation increase in the diffuse radiation values, making the instantaneous opto-electronic gain to have sudden increases, with a peak gain of 2.84 recorded at 13:45 p.m. If this result is compared with the gain of the simulations which is 2.12, it gives

a difference of 3.8%. Several factors can affect the outdoor experiment increasing or decreasing the concentration ratio: for instance the reflectivity values, which can be divided into the surrounding building's materials and colours or the ground reflection which is only considered for tilted surfaces; the location of the experiment is suitable to remove these factors from the results as the SVF is ideal. There are other aspects which affected the performance of a PV cell such as the wind, which has an influence on the cell because cells are semiconductor based, which makes them very sensitive to temperature. The average wind speed for those 6.5 h of the experiment was 2.9 m/s which is not a significant value. Rain also affects the cell efficiency since it cools down the system. Nevertheless, the data from the weather station indicates the rain rate with a value of 0 during the experiment.

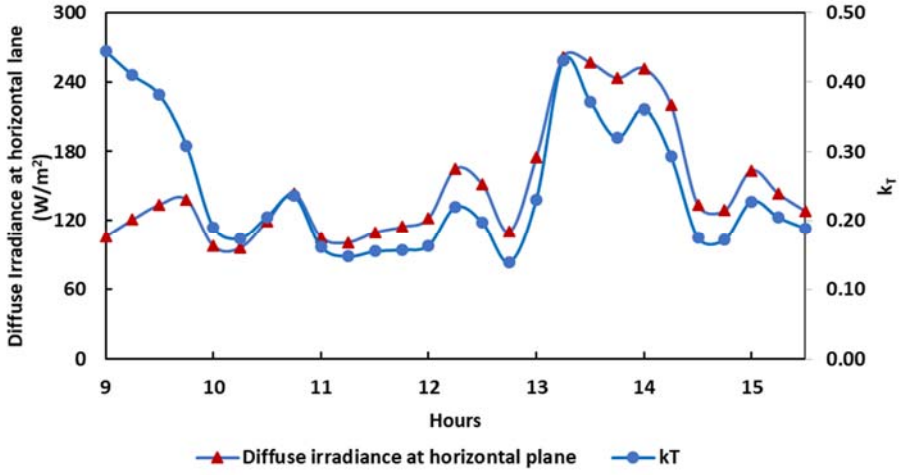

Figure 7. The k_T and diffuse irradiance at the horizontal plane values during the outdoor experiment.

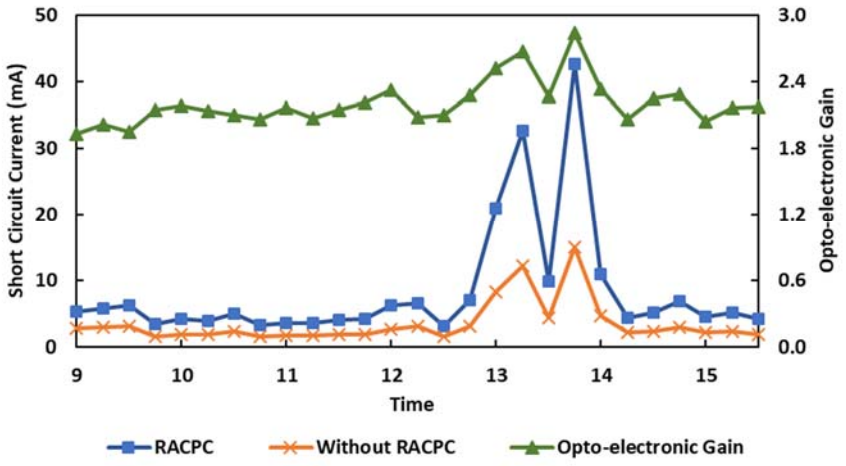

Figure 8. Results from outdoor experiments during an overcast day.

5. Conclusions

Different analyses of the performance of the RACPC for use in BIPV systems under diffuse light conditions were carried out in this project. Simulation work was carried using ZEMAX® software with the aim of determining the optical concentration gain under diffuse irradiance. The angle of incidence of the rays does not affect the results due to the fact that rays from diffuse radiation come from various directions having an optical concentration gain under diffuse irradiance of 2.12. In order to validate experimentally the results from the simulations, a single device with the RACPC-PV was integrated with a 1 cm by 1 cm solar cell. The design was tested outdoors with the aim of comparing the results obtained on an overcast day with the optical concentration gain obtained from the ZEMAX® simulation, which has a value of 2.20. This means a deviation of 3.8% in the opto-electronic gain.

The results from this work allow for more accurate way of predicting the actual annual performance of any concentrator technology, especially the RACPC installed at any location; by taking into account the contribution from both direct and diffuse radiations.

Author Contributions: Conceptualisation, S.F., R.R.-I. and D.F.R.; Data curation, S.F.; Formal analysis, S.F.; Funding acquisition, F.M.-S., R.R.-I., S.H.A.-B., N.A.B. and J.A.A.-R.; Investigation, S.F. and J.D.-G.; Methodology, F.M.-S., R.R.-I., D.F.R. and S.H.A.-B.; Resources, R.R.-I.; Software, S.F., F.M.-S., R.R.-I., D.F.R. and S.H.A.-B.; Supervision, F.M.-S., R.R.-I. and D.F.R.; Validation, F.M.-S. and R.R.-I.; Visualisation, S.F., F.M.-S. and S.H.A.-B.; Writing—original draft, S.F.; Writing—review and editing, S.F., F.M.-S., R.R.-I., D.F.R., J.D.-G., S.H.A.-B., N.A.B., A.B.M., A.A.M. and J.A.A.-R.; All authors have read and agreed to the published version of the manuscript.

Funding: The authors would like to thank Ministry of Higher Education (MOHE), Malaysia, Universiti Teknologi Malaysia (UTM) (Research cost centre no. Q.K130000.3556.06G43), the support of the Agencia Nacional de Investigación y Desarrollo (through the project Fondecyt regular 1200055 and the project Fondef ID19I10165), project PI_m_19_01 (UTFSM) and School of Computing, Engineering and Built Environment, Glasgow Caledonian University for funding this research project.

Conflicts of Interest: The authors declare no conflict of interest. The funders had no role in the design of the study; in the collection, analyses, or interpretation of data; in the writing of the manuscript, or in the decision to publish the results.

References

1. Aelenei, D.; Lopes, R.A.; Aelenei, L.; Gonçalves, H. Investigating the potential for energy flexibility in an office building with a vertical BIPV and a PV roof system. *Renew. Energy* **2019**, *137*, 189–197. [CrossRef]
2. Saretta, E.; Caputo, P.; Frontini, F. A review study about energy renovation of building facades with BIPV in urban environment. *Sustain. Cities Soc.* **2019**, *44*, 343–355. [CrossRef]
3. Kumar, N.M.; Sudhakar, K.; Samykano, M. Performance comparison of BAPV and BIPV systems with c-Si, CIS and CdTe photovoltaic technologies under tropical weather conditions. *Case Stud. Therm. Eng.* **2019**, *13*, 100374. [CrossRef]
4. Heinstein, P.; Ballif, C.; Perret-Aebi, L.-E. Building Integrated Photovoltaics (BIPV): Review, Potentials, Barriers and Myths. *Green* **2013**, *3*, 125–156. [CrossRef]
5. Chen, X.; Huang, J.; Zhang, W.; Yang, H. Exploring the optimization potential of thermal and power performance for a low-energy high-rise building. *Energy Procedia* **2019**, *158*, 2469–2474. [CrossRef]
6. Aguacil, S.; Lufkin, S.; Rey, E. Active surfaces selection method for building-integrated photovoltaics (BIPV) in renovation projects based on self-consumption and self-sufficiency. *Energy Build.* **2019**, *193*, 15–28. [CrossRef]
7. Shukla, A.K.; Sudhakar, K.; Baredar, P. Recent advancement in BIPV product technologies: A review. *Energy Build.* **2017**, *140*, 188–195. [CrossRef]
8. Polysolar. *Guide to BIPV*; Polysolar: Cambridge, UK, 2015.
9. Sharma, P.; Kolhe, M.; Sharma, A. Economic performance assessment of building integrated photovoltaic system with battery energy storage under grid constraints. *Renew. Energy* **2020**, *145*, 1901–1909. [CrossRef]
10. Solarfassade. Building-Integrated PV (BIPV). Available online: http://www.solarfassade.info/en/fundamentals/bipv/index.php (accessed on 24 October 2014).
11. The Green Age. Introduction to Solar PV. Available online: https://www.thegreenage.co.uk/tech/types-of-solar-panel/ (accessed on 29 March 2019).
12. Onyx Solar. *Projects & References*; Onyx Solar: Avila, Spain, 2017.
13. Zero Carbon Hub. *Zero Carbon Homes and Nearly Zero Energy Buildings: UK Building Regulations and EU Directives*; Zero Carbon Hub: London, UK, 2014.
14. IEA-PVPS. *Trends 2018 in Photovoltaic Applications*; IEA-PVPS: Paris, France, 2018.
15. Baig, H.; Fernández, E.F.; Mallick, T.K. Influence of spectrum and latitude on the annual optical performance of a dielectric based BICPV system. *Sol. Energy* **2016**, *124*, 268–277. [CrossRef]
16. Meng, X.; Sellami, N.; Knox, A.R.; Montecucco, A.; Siviter, J.; Mullen, P.; Ashraf, A.; Samarelli, A.; Llin, L.F.; Paul, D.J.; et al. A novel absorptive/reflective solar concentrator for heat and electricity generation: An optical and thermal analysis. *Energy Convers. Manag.* **2016**, *114*, 142–153. [CrossRef]
17. Abu-Bakar, S.H.; Muhammad-Sukki, F.; Freier, D.; Ramirez-Iniguez, R.; Mallick, T.K.; Munir, A.B.; Mohd Yasin, S.H.; Abubakar Mas'ud, A.; Abu-Bakar, S.S.; Bani, N.A.; et al. Potential of implementing the low concentration photovoltaic systems in the United Kingdom. *Int. J. Electr. Comput. Eng.* **2017**, *7*, 1398–1405. [CrossRef]

18. Abu-Bakar, S.H.; Muhammad-Sukki, F.; Freier, D.; Ramirez-Iniguez, R.; Mallick, T.K.; Munir, A.B.; Mohd Yasin, S.H.; Abubakar Mas'ud, A.; Md Yunus, N. Performance analysis of a novel rotationally asymmetrical compound parabolic concentrator. *Appl. Energy* **2015**, *154*, 221–231. [CrossRef]
19. Mammo, E.D.; Sellami, N.; Mallick, T.K. Performance analysis of a reflective 3D crossed compound parabolic concentrating photovoltaic system for building façade integration. *Prog. Photovoltaics Res. Appl.* **2013**, *21*, 1095–1103. [CrossRef]
20. Freier, D.; Muhammad-Sukki, F.; Abu-Bakar, S.; Ramirez-Iniguez, R.; Munir, A.B.; Mohd Yasin, S.H.; Bani, N.A.; Abubakar Mas'ud, A.; Ardila-Rey, J.A.; Karim, M.E. Annual prediction output of an RADTIRC-PV module. *Energies* **2018**, *11*, 544. [CrossRef]
21. Cruz-Silva, O.H.; Jaramillo, O.A.; Borunda, M. Full analytical formulation for Dielectric Totally Internally Reflecting Concentrators designs and solar applications. *Renew. Energy* **2017**, *101*, 804–815. [CrossRef]
22. Aste, N.; Buzzetti, M.; Del Pero, C.; Fusco, R.; Leonforte, F.; Testa, D. Triggering a large scale luminescent solar concentrators market: The smart window project. *J. Clean. Prod.* **2019**, *219*, 35–45. [CrossRef]
23. Gajic, M.; Lisi, F.; Kirkwood, N.; Smith, T.A.; Mulvaney, P.; Rosengarten, G. Circular luminescent solar concentrators. *Sol. Energy* **2017**, *150*, 30–37. [CrossRef]
24. Sarmah, N.; Richards, B.S.; Mallick, T.K. Design, development and indoor performance analysis of a low concentrating dielectric photovoltaic module. *Sol. Energy* **2014**, *103*, 390–401. [CrossRef]
25. Mallick, T.; Eames, P. Design and fabrication of low concentrating second generation PRIDE concentrator. *Sol. Energy Mater. Sol. Cells* **2007**, *91*, 597–608. [CrossRef]
26. Dayanand, A.; Aykapadathu, M.; Sellami, N.; Nazarinia, M. Experimental investigation of a novel absorptive/feflective solar concentrator: A thermal analysis. *Energies* **2020**, *13*, 1281. [CrossRef]
27. Abu-Bakar, S.H.; Muhammad-Sukki, F.; Freier, D.; Ramirez-Iniguez, R.; Mallick, T.K.; Munir, A.B.; Mohd Yasin, S.H.; Abubakar Mas'ud, A.; Bani, N.A. Performance analysis of a solar window incorporating a novel rotationally asymmetrical concentrator. *Energy* **2016**, *99*, 181–192. [CrossRef]
28. Marín-Sáez, J.; Chemisana, D.; Moreno, Á.; Riverola, A.; Atencia, J.; Collados, M.-V. Energy simulation of a holographic PVT concentrating system for building integration applications. *Energies* **2016**, *9*, 577. [CrossRef]
29. Timmermans, G.H.; Douma, R.F.; Lin, J.; Debije, M.G. Dual thermal-/tlectrical-responsive luminescent 'smart' window. *Appl. Sci.* **2020**, *10*, 1421. [CrossRef]
30. Aghaei, M.; Nitti, M.; Ekins-Daukes, N.J.; Reinders, A.H.M.E. Simulation of a novel configuration for luminescent solar concentrator photovoltaic devices using bifacial silicon solar cells. *Appl. Sci.* **2020**, *10*, 871. [CrossRef]
31. IRENA. *Renewable Energy Technologies: Cost Analysis Series-Solar Photovoltaics*; IRENA: Abu Dhabi, UAE, 2012.
32. Abu-Bakar, S.H.; Muhammad-Sukki, F.; Ramirez-Iniguez, R.; Mallick, T.K.; Munir, A.B.; Mohd Yasin, S.H.; Abdul Rahim, R. Rotationally asymmetrical compound parabolic concentrator for concentrating photovoltaic applications. *Appl. Energy* **2014**, *136*, 363–372. [CrossRef]
33. Abu-Bakar, S.H. Novel Rotationally Asymmetrical Solar Concentrator for the Building Integrated Photovoltaic System. Ph.D Thesis, Glasgow Caledonian University, Glasgow, UK, 2016.
34. Freier, D. Software Simulation and Experimental Characterisation of a MSDTIR Concentrator for BIPV Systems under Direct and Diffuse Solar Radiation. Bachelor's Thesis, University of Applied Sciences, Berlin, Germany, 2014.
35. Hämmerle, M.; Gál, T.; Unger, J.; Matzarakis, A. Introducing a script for calculating the sky view factor used for urban climate investigations. *Acta Climatol. Chorol.* **2011**, *44–45*, 83–92.
36. Davis Instruments. Wireless Vantage Pro2 & Vantage Pro2 Plus Station. Available online: https://www.weathershop.co.uk/shop/davis-vantage-pro2-plus-fars-weather-station (accessed on 29 March 2019).
37. Quaschning, V. *Understanding Renewable Energy Systems*, 1st ed.; Earthscan: Bath, UK, 2005; ISBN 1-84407-128-6.